Hydrodynamic analysis of the piston mode resonance inside a large FLNG turret

B. Molin[1], I. de Vries[2], A. Cinello[3]

[1] Aix Marseille Université, CNRS, Centrale Marseille, IRPHE UMR 7342, 13451 Marseille cedex 20, France (bernard.molin@centrale-marseille.fr)

[2] SBM Offshore, BP 199, MC 98007 Monaco cedex

[3] Océanide, BP 63, 83502 la Seyne sur mer, France

The FLNG under construction in South-Korea by Samsung Heavy Industry (SHI) will be the world largest floating facility, with a length of 488 meters and a displacement over 600 000 tons. It will be installed off the western coast of Australia. Other FLNG projects are coming up. All these FLNG are moored by turrets with typical diameter size in the range 25-30 m.

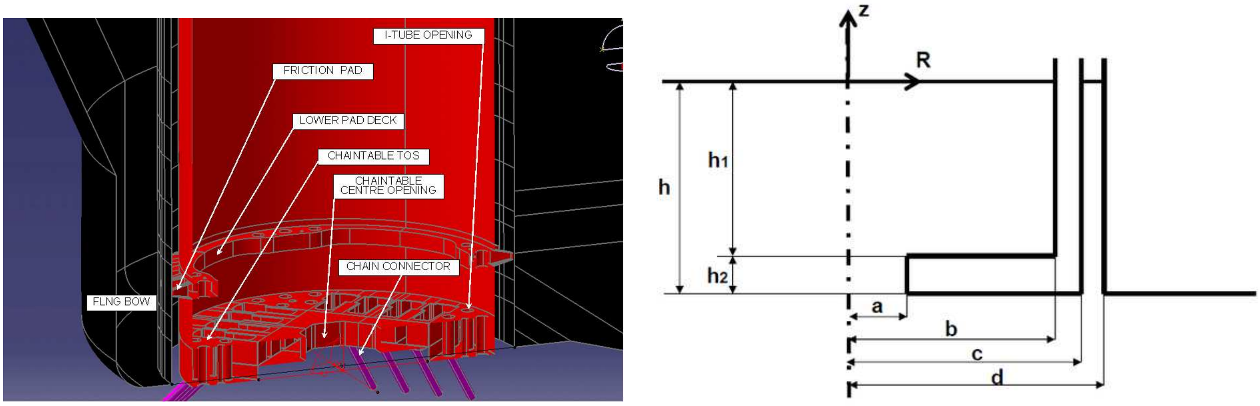

Figure 1: Conceptual view of the turret and idealization.

Figure 1 shows some details of the FLNG turret: it is alike a truncated cylinder, fitted inside a moonpool. The cylinder bottom (the chaintable) has a major central opening and several peripheral ones, to give way to the anchor chains and to the risers. Also noteworthy is the about 2 meter wide space in-between the turret and the moonpool walls.

An hydrodynamic issue associated with the turret is the occurrence of resonant sloshing motion under excitation from the outer waves, and more particularly the combined piston modes occurring inside the turret and in the annular space in-between the turret and the moonpool walls.

In this paper we present a simple approximate model, based on linearized potential flow theory, to determine the combined natural modes in the turret and in the annular space. We also present some results from dedicated model tests, where from it appears that, as a result of flow separation through the chain table openings, the turret piston mode is heavily damped.

Semi-analytical model

The considered geometry is shown in figure 1: it is assumed to be axisymmetric, with the perforations through the chaintable reduced to a single central opening of radius a: the "restriction" following the terminology used by Sphaier *et al.* (2007). Similar simplifying assumptions as in Molin (2001) are made: the FLNG hull is idealized as an infinite motionless horizontal wall and the masses of water, inside the annulus, and inside the restriction (for $0 \leq R \leq a$ and $-h \leq z \leq -h_1$), are "frozen".

The heave motions for the frozen water inside the restriction (z_1) and inside the annulus (z_2)

obey the following coupled equations:

$$\left[\rho\,\pi\,a^2\,h_2 + m_{10} + m_{11}\right]\ddot{z}_1 + m_{12}\,\ddot{z}_2 + \rho\,g\,\pi\,\frac{a^4}{b^2}\,z_1 = 0 \tag{1}$$

$$\left[\rho\,\pi\,(d^2-c^2)\,h + m_{22}\right]\ddot{z}_2 + m_{21}\,\ddot{z}_1 + \rho\,g\,\pi\,(d^2-c^2)\,z_2 = 0 \tag{2}$$

with m_{10} the added mass due to the entrapped water inside the turret (above the frozen restriction), and m_{ij} $(i=1,2;\ j=1,2)$ the added masses due to the lower fluid domain.

It can be noted that the problem studied here has some similarity with Newman (2003) or Miles (2002).

Turret added mass

To determine the added mass m_{10} one must solve the following boundary value problem:

$$\begin{array}{rcllr}
\Delta\varphi & = & 0 & 0 \le R \le b & -h_1 \le z \le 0 \qquad (3)\\
\varphi_R & = & 0 & R = b & -h_1 \le z \le 0 \qquad (4)\\
\varphi_z & = & 1 & 0 \le R \le a & z = -h_1 \qquad (5)\\
\varphi_z & = & 0 & a \le R \le b & z = -h_1 \qquad (6)\\
g\,\varphi_z - \omega^2\,\varphi & = & 0 & 0 \le R \le b & z = 0 \qquad (7)
\end{array}$$

The velocity potential φ can be looked for under the form

$$\varphi(R,z) = A_0\,z + B_0 + \sum_{n=1}^{\infty}\left[A_n\,\frac{\sinh\lambda_n z}{\cosh\lambda_n h_1} + B_n\,\frac{\cosh\lambda_n(z+h_1)}{\cosh\lambda_n h_1}\right]\,J_0(\lambda_n R) \tag{8}$$

where J_0 is the standard Bessel function and λ_n are the roots of

$$J_0'(\lambda_n b) = -J_1(\lambda_n b) = 0 \tag{9}$$

In this way the Laplace equation and the no-flow condition (4) at the vertical wall $R=b$ are fulfilled. From the free surface condition (7) the following relationships between B_n and A_n are derived:

$$B_0 = \frac{A_0\,g}{\omega^2} \qquad\qquad B_n = \frac{A_n}{\cosh\lambda_n h_1}\,\frac{g\,\lambda_n}{\omega^2 - g\,\lambda_n\,\tanh\lambda_n h_1} \tag{10}$$

The no-flow conditions (5) and (6) in $z=-h_1$ remain to be fulfilled. From the orthogonality of the $J_0(\lambda_n R)$ functions over $[0\ b]$ the following is obtained:

$$A_0 = \frac{a^2}{b^2} \qquad\qquad A_n = \frac{2\,a}{\lambda_n^2\,b^2}\,\frac{J_1(\lambda_n a)}{J_0^2(\lambda_n b)} \tag{11}$$

Finally the added mass m_{10} is obtained as

$$m_{10} = \frac{\rho\,\pi\,a^4\,h_1}{b^2} - 2\,\pi\,\rho\,a\,\sum_{n=1}^{\infty}\frac{C_n}{\lambda_n}\,J_1(\lambda_n a) \tag{12}$$

where

$$C_n = -A_n\,\tanh\lambda_n h_1 + \frac{B_n}{\cosh\lambda_n h_1} \tag{13}$$

while the B_0 term yields the hydrostatic stiffness $\rho\,g\,\pi\,a^4/b^2$.

From equation (10), the coefficients B_n, and consequently the added mass, depend on the frequency ω. In the case considered here where the height h_1 is larger than the radius b, the frequency dependence turns out to be hardly noticeable. (An associated result is that the free surface remains flat when the water volume inside the turret heaves up and down.)

Added masses from the lower fluid domain

As written earlier the lower fluid domain is assumed to be semi-infinite, bounded in $z = -h$ by an infinite horizontal wall. It results that the added mass m_{11} is given by

$$m_{11} = \frac{\rho}{2\,\pi} \iint_{S_1} \iint_{S_1} \frac{1}{PQ} \, \mathrm{d}S_P \, \mathrm{d}S_Q = -\frac{\rho}{2\,\pi} \int_{C_1} \int_{C_1} PQ \, \overrightarrow{n_P} \cdot \overrightarrow{n_Q} \, \mathrm{d}l_P \, \mathrm{d}l_Q \tag{14}$$

with S_1 the disc $0 \leq R \leq a$, C_1 its perimeter and $\overrightarrow{n_P}$, $\overrightarrow{n_Q}$ the outward normal vectors in P and Q. One obtains $m_{11} = 8\,\rho\,a^3/3$ as it is well known.

Likewise the added mass m_{22}, associated with the solid heave motion of the water entrapped within the annular space, is given by

$$m_{22} = -\frac{\rho}{2\,\pi} \int_{C_2} \int_{C_2} PQ \, \overrightarrow{n_P} \cdot \overrightarrow{n_Q} \, \mathrm{d}l_P \, \mathrm{d}l_Q \tag{15}$$

where the contour C_2 consists in the two circles $R = c$ and $R = d$. One obtains:

$$m_{22} = \frac{8}{3}\,\rho\,d^3 \left(1 + r^3 + \frac{3}{2}\,r\,\sqrt{1+r^2}\,I(r)\right) \tag{16}$$

with $r = c/d$, $k = 2\,r/(r^2+1)$ and

$$I(r) = \int_0^{\pi} \cos\psi \, \sqrt{1 - k\,\cos\psi} \, \mathrm{d}\psi \tag{17}$$

$I(r)$ can be written down as a complicated expression of elliptic integrals. It is more straightforward and safer to evaluate it numerically.

Finally the cross added mass $m_{12} = m_{21}$ is obtained as

$$m_{12} = -\frac{\rho}{2\,\pi} \int_{C_1} \int_{C_2} PQ \, \overrightarrow{n_P} \cdot \overrightarrow{n_Q} \, \mathrm{d}l_P \, \mathrm{d}l_Q = -2\,\rho\,a\,d\,\sqrt{a^2+d^2}\,I(a/d) + 2\,\rho\,a\,c\,\sqrt{a^2+c^2}\,I(a/c) \tag{18}$$

Illustrative results

Some model tests were carried out in the experimental facilities of Océanide. We take the same geometry here, that is $b = 0.155$ m, $c = 0.156$ m, $d = 0.177$ m, $h_1 = 0.272$ m, $h_2 = 0.028$ m, and we vary the radius of the restriction a.

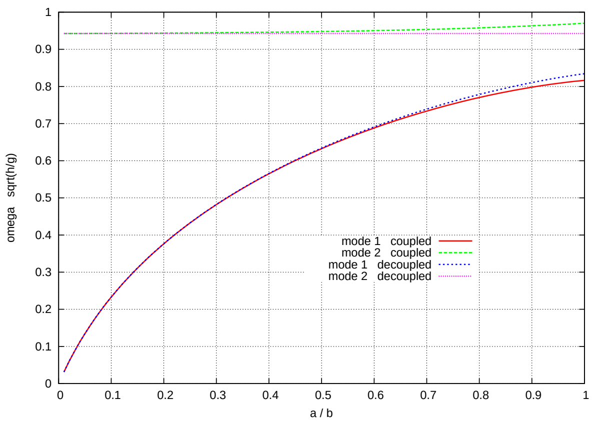

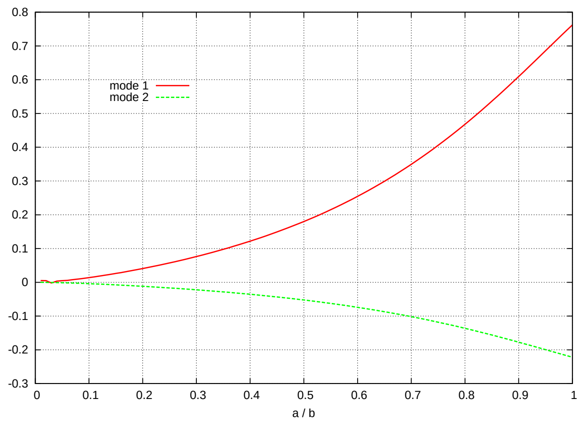

Figure 2: Natural frequencies $\omega_i\,\sqrt{h/g}$(left) and alternate component of the eigen vector vs a/b.

Figure 2 shows the non-dimensional natural frequencies $\omega_i\,\sqrt{h/g}$ where $h = h_1 + h_2$ (left) and, for each mode, the alternate component of the eigen vector, the other one being equal to one (right). When a/b is small, the alternate component is nearly zero, meaning that the piston resonances in the turret and in the annulus are decoupled. It can be observed, from figure 2 that the natural frequency of the turret piston mode goes to zero as a/b goes to zero. (It has been checked that our formulas give natural frequencies in good agreement with the experimental values reported by Sphaier *et al.* (2007) in the case of their MONOBR platform.)

As a/b increases the piston mode resonances become coupled. For instance, for $a/b = 0.75$, the alternate components of the eigen vectors take the values 0.406 and -0.118. This means that when the turret resonates at frequency ω_1 with a unit amplitude of the free surface motion (in figure 2 the reference is the vertical motion of the free surface), the annulus resonates at the same frequency with 0.406 amplitude, in phase. When the annulus resonates at frequency ω_2 with a unit amplitude, the free surface inside the turret oscillates with an amplitude 0.118 and out of phase.

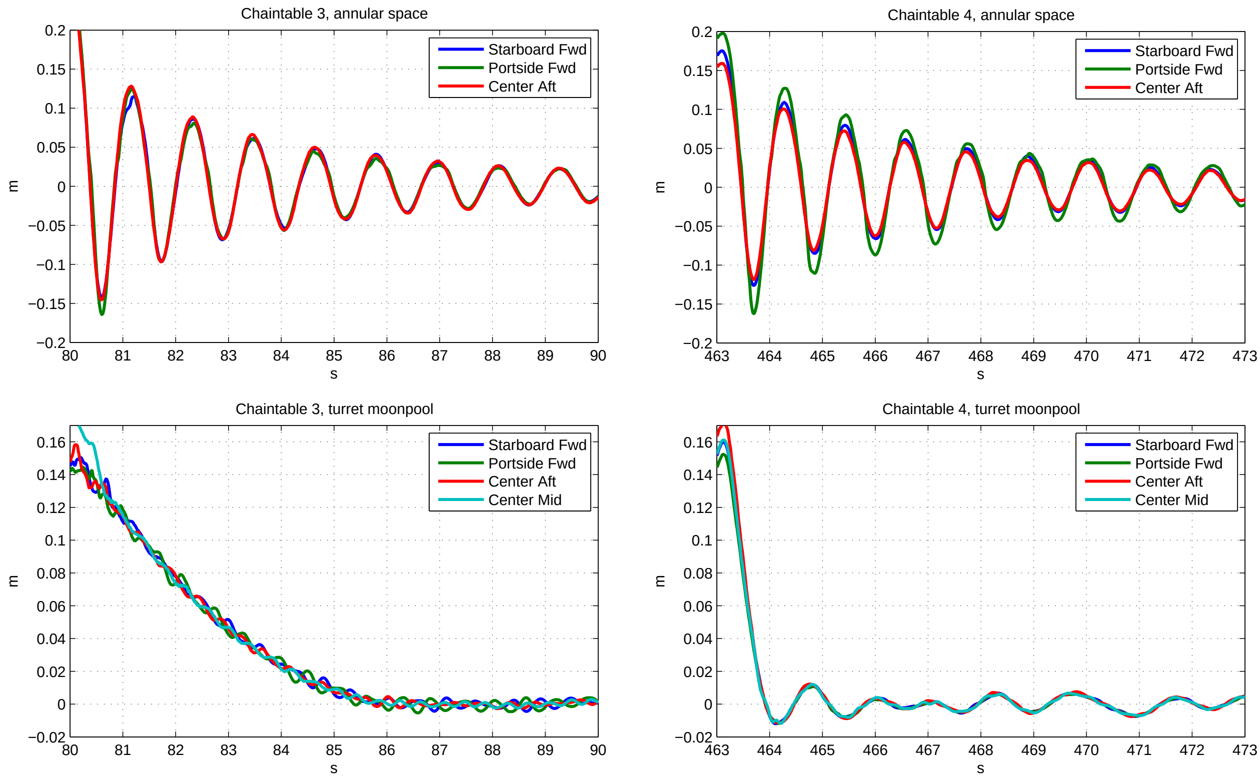

Figure 3: Time series of the decay tests for chaintables 3 and 4.

Finally figure 3 shows time series from decay tests with two of the tested chaintable models. Chaintable 3 has just one central opening with an a/b ratio of 0.17. Chaintable 4 has the same central opening and additional peripheral openings that, on a standpoint of total open area, are "equivalent" to a central opening with $a/b = 0.47$. The signals are from different wave gauges inside the annular space (top) and inside the turret (bottom). Initial displacements from the free surfaces were achieved through air depressurizing in a chamber set on top, which was abruptly opened. It is striking that, in the case of chaintable 3, the viscous damping, occurring from flow separation, is more than critical: no oscillation can be seen. The oscillation frequencies agree fairly well with the predictions from figure 2.

Permission to publish by SBM Offshore is gratefully acknowledged by the authors.

References

MILES J. 2002 On slow oscillations in coupled wells, *J. Fluid Mech.*, **455**, 283–287.

MOLIN B. 2001 On the piston and sloshing modes in moonpools, *J. Fluid Mech.*, **430**, 27–50.

NEWMAN J.N. 2003 Low-frequency resonance of moonpools, *Proc. 18th International Workshop on Water Waves and Floating Bodies*, le Croisic.

SPHAIER S.H., TORRES F.G.S., MASETTI I.Q., COSTA A.P. & LEVI C. 2007 Monocolumn in waves: Experimental analysis, *Ocean Engineering*, **34**, 1724–1733.